Research Paper

Spatial transcriptomic analysis of adult hippocampal neurogenesis in the human brain

Sophie Simard, BSc; Reza Rahimian, PharmD, PhD; Maria Antonietta Davoli, MSc; Stéphanie Théberge, MSc; Natalie Matosin, PhD; Gustavo Turecki, MD, PhD; Corina Nagy, PhD; Naguib Mechawar, PhD

Background: Adult hippocampal neurogenesis has been extensively characterized in rodent models, but its existence in humans remains controversial. We sought to assess the phenomenon in postmortem human hippocampal samples by combining spatial transcriptomics and multiplexed fluorescent in situ hybridization. **Methods:** We computationally examined the spatial expression of various canonical neurogenesis markers in postmortem dentate gyrus (DG) sections from young and middle-aged sudden-death males. We conducted in situ assessment of markers expressed in neural stem cells, proliferative cells, and immature granule neurons in postmortem DG sections from infant, adolescent, and middle-aged males. **Results:** We examined frozen DG tissue from infant (n = 1, age 2 yr), adolescent (n = 1, age 16 yr), young adult (n = 2, mean age 23.5 yr), and middle-aged (n = 2, mean age 42.5 yr) males, and frozen-fixed DG tissue from middle-aged males (n = 6, mean age 43.5 yr). We detected very few cells expressing neural stem cell and proliferative markers in the human DG from childhood to middle age. However, at all ages, we observed a substantial number of DG cells expressing the immature neuronal marker *DCX*. Most *DCX*$^+$ cells displayed an inhibitory phenotype, while the remainder were non-committed or excitatory in nature. **Limitations:** The study was limited by small sample sizes and included samples only from males. **Conclusion:** Our findings indicate very low levels of hippocampal neurogenesis throughout life and the existence of a local reserve of plasticity in the adult human hippocampus. Overall, our study provides important insight into the distribution and phenotype of cells expressing neurogenesis markers in the adult human hippocampus.

Introduction

Occurrence of adult hippocampal neurogenesis in the subgranular zone of the human dentate gyrus (DG) was first suggested around 25 years ago.[1] Adult hippocampal neurogenesis in the human brain has been extensively investigated, but mainly with immunohistochemical approaches, yielding highly discordant conclusions.[2–9] The controversy in the literature regarding the extent to which adult hippocampal neurogenesis occurs in the human brain can be attributed to a wide range of factors, including differences in the brain specimens[10–12] and the immunohistochemistry protocols used to identify neurogenic cell types,[4,13] specifically the antibodies used to define neurogenesis in the human DG.[11]

These differences have ultimately resulted in diverging conclusions regarding different neurogenic cells immunolabelled in the adult human hippocampus. For instance, doublecortin (DCX) antibodies have been extensively used in various immunohistochemical studies to characterize immature granule neurons in the neurogenic niche. However, the presence of DCX-immunolabelled cells in the DG has been under intense debate, with studies reporting contradictory levels of DCX expression in the DG during physiologic aging.[2,3,5,7,8,9,13,14] Although studies examining the expression of neurogenesis and proliferative markers in the adult human hippocampus with in situ hybridization are still lacking, Tartt and colleagues[15] found that density of cells positive for *DCX* mRNA in the adult neurotypical human hippocampus did not decline with age, which was comparable to their findings related to DCX-immunolabelled cells, therefore suggesting some agreement in protein and mRNA expression levels. More recently, a proliferation of studies have used single-cell and single-nucleus RNA sequencing to examine adult hippocampal neurogenesis at the transcriptomic level.[16–20] Although these methods provide transcriptomic signatures for different cell types detected in the DG, they lack spatial resolution. In addition, as recently reviewed by our group,[21] some studies have identified a neurogenic lineage trajectory in their data sets,

Correspondence to: N. Mechawar, McGill Group for Suicide Studies, Douglas Mental Health University Institute, Department of Psychiatry, McGill University, 6875 Boulevard LaSalle, Verdun, Que., H4H 1R3; naguib.mechawar@mcgill.ca.

Submitted Mar. 8, 2024; Revised June 21, 2024; Accepted Aug. 18, 2024

Cite as: *J Psychiatry Neurosci* 2024 October 16;49(5). doi: 10.1503/jpn.240026

while others have not. These discrepancies may be explained by the differences in the methodological and computational approaches used in these single-nucleus genomic studies.

In the present study, we sought to assess the spatial expression of various neurogenesis-related genes in the adult human DG at the transcriptomic level using spatial transcriptomic tools and multiplexed fluorescent in situ hybridization (FISH). Although single-molecule in situ hybridization has been used in the context of adult hippocampal neurogenesis in the human brain,[7,15] these studies looked only at *DCX* mRNA–expressing cells and did not investigate their phenotype. Here, we sought to integrate spatial transcriptomics and multiplexed FISH to characterize, both computationally and in situ, the spatial expression of markers commonly used in the literature to identify neurogenic cell types in the DG at the transcriptomic level.

Methods

Human postmortem tissue

We obtained frozen DG tissue from well-characterized adolescent, young adult, and middle-aged males, and frozen-fixed DG tissue from middle-aged males from the Douglas-Bell Canada Brain Bank (Montréal, Canada). In collaboration with the Quebec Coroner's Office and with informed consent from next of kin, phenotypic information was obtained with standardized psychological autopsies. Presence of any or suspected neurologic or neurodegenerative disorder signalled in clinical files constituted an exclusion criterion. Sudden-death controls — people who died by natural or accidental causes of death, without any brain disorder — are defined with the support of medical charts and coroner records. Toxicological assessments and medication prescription were also obtained. The samples used for spatial transcriptomic experiments were dissected from the anterior hippocampus and the body (close to the anterior pole) of the hippocampus, while all frozen-fixed samples used for RNAscope were dissected from the anterior hippocampus. We obtained an infant frozen DG sample from Dr. Nada Jabado's laboratory at The Research Institute of the McGill University Health Centre. Detailed information on the samples used for spatial transcriptomic and FISH experiments is in Appendix 1, Tables 1 and 2, available at www.jpn.ca/lookup/doi/10.1503/jpn.240026/tab-related-content.

Tissue processing and spatial transcriptomic data generation

Frozen tissue embedded in optimal cutting temperature compound was cryosectioned at –20°C. We placed sections of 10-µm thickness in the 6.5-mm by 6.5-mm fiducial frame capture area of Visium Spatial Gene Expression Slides (no. 2000233, 10x Genomics) to maximize tissue coverage. Next, we fixed the tissue sections in methanol at –20°C for 30 minutes and stained them with hematoxylin and eosin according to the Visium Spatial Gene Expression User Guide (CG000239, 10x Genomics). The tissue was permeabilized for 12 minutes based on tissue optimization time-course experiments. We took bright-field images using the Olympus VS120 slide scanner with a 10× objective and exported them as low-resolution and high-resolution TIFF files. Libraries were prepared according to the Visium Spatial Gene Expression User Guide and loaded at 300 pM. We sequenced libraries on a NovaSeq 6000 System (Illumina) using a NovaSeq S4 Reagent Kit (200 cycles, no. 20027466, Illumina), at very high sequencing depths ranging between 290 and 420 × 10^6 read-pairs per sample. The protocol for sequencing involved 28 cycles for read 1, 10 cycles for the i7 index read, 10 cycles for the i5 index read, and 90 cycles for read 2.

Spatial transcriptomic data processing

To process the sequenced data, we used the 10x Genomics analysis pipeline Space Ranger (spaceranger-1.1.0 version) to create FASTQ files, which we mapped to the 10x Genomics GRCh38 reference human genome (GRCh38–2020-A) for gene quantification. Quality control metrics returned by this software are presented in Appendix 1, Table 1. We used the Space Ranger count pipeline to generate output files, including feature barcode matrices; Loupe Browser files for data visualization; a data summary with images, metrics, and plots; downsampled input images; and spot barcode locations for downstream analysis.

Manual annotation

We manually annotated each section on LoupeBrowser (version 5.0.0), the 10x Genomics Visium data visualization software, by assigning each spot to a specific region of the DG. The manual annotations were done based on the human anatomic atlas from the Allen Brain Atlas[22] and validated by a blinded histology expert. After manual annotation, 7 clusters were defined on each section.

Clustering accuracy comparison and unsupervised spot clustering

The Space Ranger outputs of each sample were read into R (version 4.1.0; RRID:SCR_001905)[23] in a customized structure using the Seurat R package[24] (version 4.1.1) to keep them paired with the low-resolution histology images for visualization. A detailed description of the steps used for the quality check and preprocessing of the data are included in Appendix 1.

We exported and integrated the manual annotations in the merged Seurat object for a comparison between the clustering performance of 4 different clustering algorithms, namely kmeans with the R package stats,[23] mclust with the R package mclust (version 5.4.7),[25] BayesSpace normal error method, and BayesSpace *t*-distributed error method.[26] The clustering resolution was set at 7 clusters for each algorithm as there were 7 manually annotated clusters in each section. The clustering accuracy for each algorithm was assessed using the adjusted rand index, as previously described.[26,27] Based on this index, we performed unsupervised clustering using the BayesSpace (*t*-distributed error model) clustering

algorithm (version 1.4.1) with the *spatialCluster* (50 000 Markov chain Monte Carlo iterations [nrep]) BayesSpace function (Appendix 1, Supplementary Figure 1). We used Seurat for clustering visualization using the *SpatialPlot* function. We assessed the average expression of different canonical cell type markers in each BayesSpace cluster from all sections by generating a dotplot with the *DotPlot* function from Seurat. We used well-known cell-type markers for dotplot visualization, namely *SATB2*, *SLC17A7*, and *SLC17A6* (excitatory neurons); *GAD1* and *GAD2* (inhibitory neurons); *TMEM119*, *CX3CR1*, and *MRC1* (microglia); *CLDN5* and *VTN* (endothelial cells); *GLUL*, *SOX9*, *AQP4*, *GFAP*, *ALDH1L1*, and *VIM* (astrocytes); *PDGFRA*, *OLIG1*, and *OLIG2* (oligodendrocyte precursor cells); *PLP1*, *MOG*, *MOBP*, and *MBP* (oligodendrocytes); and *SNAP25*, *STMN2*, and *RBFOX3* (neurons).

Sub-spot level analysis

We next used the *spatialEnhance* (nrep = 200 000) and *enhanceFeatures* functions of BayesSpace to computationally map the neurogenic features at the sub-spot level, where each Visium spot was divided into 6 sub-spots with BayesSpace. Although Visium spots may contain up to 30 cells, given their 55-µm diameter, each of the generated sub-spots represented the transcriptomic signatures of a lower number of cells, thus increasing the cellular resolution of the data. The default nonlinear regression model (XGBoost) was trained for each neurogenic marker to determine the gene expression measured at the spot level (maximum number of boosting iterations [nrounds] set to 0). We used the fitted model to measure gene expression with the enhanced clustering. The spatial feature plots were generated using the *featurePlot* function from BayesSpace.

For the sub-spot level analysis of a mouse Visium data set, we downloaded a publicly available data set through the 10x Genomics website (https://www.10xgenomics.com/datasets/adult-mouse-brain-section-1-coronal-stains-dapi-anti-neu-n-1-standard-1-1-0), which we then pre-processed and computed at enhanced resolution with the integrated workflow of BayesSpace (version 1.4.1). One sample from an adult mouse was included in the analysis (Appendix 1, Supplementary Figure 2).

For the sub-spot level analysis of the data set from Maynard and colleages,[27] we downloaded the publicly available data set of dorsolateral prefrontal cortex (DLPFC) spatial transcriptomic data through the spatialLIBD R package (samples 151671, 151672, 151673, 151674),[28] which we then preprocessed, batch corrected, and computed at enhanced resolution with the integrated workflow of BayesSpace (version 1.4.1).

Differential gene expression analysis

We identified differentially expressed genes (DEGs) for each BayesSpace cluster using Seurat's *FindAllMarkers* function, with the 2-sided Wilcoxon rank-sum test (adjusted [false discovery rate] $p < 0.05$ and log fold-change threshold > 0.25). We included the top 5 DEGs for each cluster in a dotplot for visualization (Appendix 1, Supplementary Figure 3A). The DEGs extracted from each BayesSpace cluster are included in Appendix 2, Table 1. We created Venn diagrams using an online tool (https://bioinfogp.cnb.csic.es/tools/venny/index.html).[29]

Spot deconvolution with single-nucleus RNA sequencing

We downloaded the publicly available human hippocampal data set from Habib and colleagues (https://www.gtexportal.org/home/datasets).[18] We performed spot deconvolution using the SPOTlight package's seeded non-negative matrix factorization regression model (version 0.1.7) in R,[30] which determined the topic profiles (i.e., the set of defining genes) within each cell type from the single-nucleus RNA sequencing data set and within each capture spot. We found the marker genes in each cluster of the data set using the *FindAllMarkers* function (with Wilcoxon rank-sum test) with Seurat. We applied the *spotlight_deconvolution* function with the standard parameters from SPOTlight to determine the topic profiles from the single-nucleus data set that best fit each spot's topic profile. The deconvolution was next assessed by looking at how specific the topic profiles were for each cell type from the single-nucleus RNA sequencing data set (Appendix 1, Supplementary Figure 4). We used the *SpatialFeaturePlot* function from Seurat to view the predicted proportions of cell-type markers of all single-nucleus RNA sequencing clusters on the spatial data (Appendix 1, Supplementary Figure 5).

Gene signature scoring

We used gene sets from Zhong and colleagues,[31] Zhou and colleagues,[20] and Wang and colleagues[19] to calculate gene enrichment scores, grouped by the BayesSpace clusters of the Visium data. We used Seurat's *AddModuleScore* function to calculate the average expression of each gene set, subtracted with the average gene expression of a set of randomly chosen control genes (number of bins [nbin] = 24 and number of control features [ctrl] = 100). We then spatially mapped the module scores directly onto each Visium section and created the corresponding violin plots using Seurat's *SpatialFeaturePlot* and *VlnPlot* functions (Appendix 1, Supplementary Figure 6). The gene sets used for gene signature scoring are included in Appendix 2, Tables 2 and 3, available at www.jpn.ca/lookup/doi/10.1503/jpn.240026/tab-related-content.

Multiplexed fluorescent in situ hybridization and data quantification

We performed FISH using Advanced Cell Diagnostics RNAscope probes and reagents (RNAscope Multiplex Fluorescent V2 Assay, ACD Bio), following the manufacturer's instructions. We conducted experiments on both frozen and frozen-fixed DG samples. Detailed information on the RNAscope experiments and the probes is provided in Appendix 1.

The slides were imaged at 20× magnification using the Olympus VS120 virtual slide scanner. We transferred the scans to QuPath[32] (version 0.3.0; RRID:SCR_018257) for

further analysis. Using QuPath's automated cell detection based on 4′,6-diamidino-2-phenylindole (DAPI) staining and manual counting, we counted the percentage of cells positive for different combinations of neurogenic markers in 2 layers of interest, the granule cell layer and subgranular zone. For each section, the granule cell layer was traced based on the DAPI staining, demonstrating a tightly compact layer of DG granule neurons; the subgranular zone was defined as a 50-µm region below the granule cell layer, as previously done by Seki and colleagues.[6] For stringent quantification, we counted cells with 4 or more fluorescent puncta as positive for *GAD1*, *NEUROD1*, *CALB2*, *NES*, *SOX2*, *TMEM119*, *ALDH1L1*, *MBP*, or *DCX* probes and labelled cells with at least 6 fluorescent puncta as positive for *SLC17A7*, *PROX1*, *PCNA*, *MCM2*, or *STMN1*. We plotted the data using the ggplot2 (version 3.3.5) R package[33] and in GraphPad (version 7). Detailed information on statistical analyses performed on the RNAscope data are included in Appendix 1.

Image acquisition

We took images using a FV1200 laser scanning confocal microscope using 20× (numerical aperture = 0.75) and 40× objective (numerical aperture = 0.95). The *X*–*Y* axis pixel number (1600 × 1600), Kalman averaging (2), and laser scanning speed (2 µs/pixel) were modified to improve image resolution. We adjusted laser power and detection voltage parameters between subjects for each set of experiments to improve image quality. All parameters were optimized to decrease the signal-to-noise ratio and remove autofluorescence from lipofuscin and cellular debris.

Results

We examined frozen DG tissue from infant (n = 1, age 2 yr), adolescent (n = 1, age 16 yr), young adult (n = 2, mean age 23.5 yr), and middle-aged (n = 2, mean age 42.5 yr) males, and frozen-fixed DG tissue from middle-aged males (n = 6, mean age 43.5 yr).

Spatial mapping of neurogenesis markers at the sub-spot level

We contextualized the spatial profiles of neurogenesis markers in the human hippocampus using frozen hippocampal sections from young and middle-aged neurotypical adults (Figure 1 and Appendix 1, Table 1). We performed unsupervised clustering on the spots in each DG section (Figure 2A and 2B and Appendix 1, Supplementary Figure 1A, 1B, and 1C and Table 3). The morphology of the DG in each sample was validated using both hematoxylin and eosin staining and FISH with a probe directed against *PROX1*, a DG-enriched gene (Figure 2C).[34] We assessed the expression levels of canonical cell-type markers for each cluster and observed their concordance with the expected spatial location of the clusters within the hippocampus (Figure 2D). Interestingly, a subset of spots in cluster 5 (56.3% of spots) located within the granule cell layer of each section, expressed the inhibitory neuronal marker *GAD1*, alongside high levels of expression of *SLC17A7*, an excitatory neuronal marker (Appendix 1, Table 4).

We next sought to spatially map markers expressed in neural stem cells, proliferative progenitor cells, neuroblasts, immature granule neurons, mature granule neurons, and cells from the dentate lineage on each section at the sub-spot level

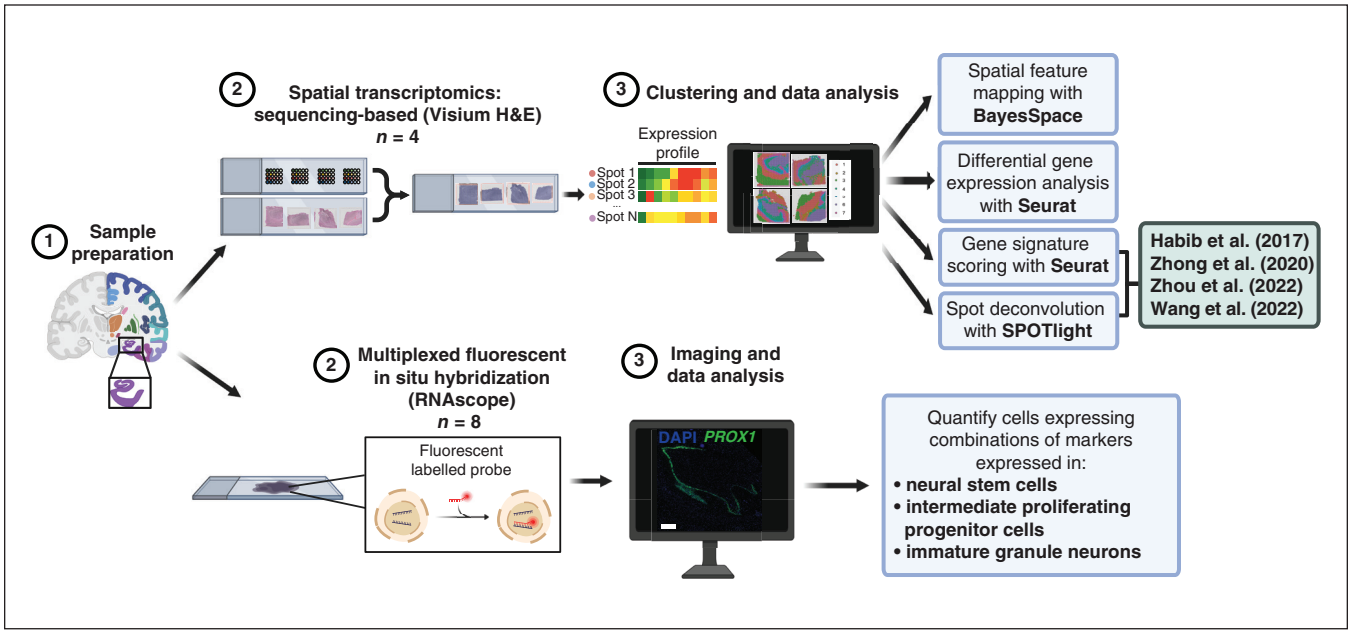

Figure 1: Schematic overview of the experimental workflow used for the spatial transcriptomic analysis of 4 hippocampal samples with 10x Genomic Visium and of 8 hippocampal samples with multiplexed fluorescent in situ hybridization (RNAscope). Figure created with BioRender (www.biorender.com). See Related Content tab for accessible version. DAPI = 4′,6-diamidino-2-phenylindole; H&E = hematoxylin and eosin.

(Figure 3). We observed *NEUROD1* expression in neuronal clusters, mainly the *PROX1*-enriched granule cell layer, which corroborated previous findings of Prox1$^+$ and NeuroD1$^+$ immunolabelled cells in the rodent DG[35] and our spatial feature mapping of *Neurod1* expression in a publicly available Visium data set of the mouse brain (Appendix 1, Supplementary Figure 2). Although many of the neurogenesis markers were expressed in either the subgranular zone or granule cell layer, the proliferative marker genes *PCNA* and *MCM2* displayed very low expression in all samples (Figure 3). Similarly, in the mouse brain, the DG exhibited lower levels of *Pcna* and *Mcm2* than in other regions of the brain (Appendix 1, Supplementary Figure 2). Moreover, *DCX* showed dispersed expression within the DG, and was also detected in hippocampal regions outside of the DG (Figure 3). Of note, we expected to find neural stem cell markers outside of the DG since there are similarities between the transcriptomic profiles of human neural stem cells and astrocytes.[36] Moreover, *NES* was expressed in sub-spots enriched for oligodendrocyte precursor cell–specific markers (Figure 2D and Figure 3), indicating possible similarities between the transcriptomic signatures of both cell types. This finding specifically emphasizes the difficulty in distinguishing transcriptomic signatures of neural stem cells from glial cells in the human DG with computational approaches that are not appropriately designed to capture rare neurogenic cell types. Finally, since we detected *GAD1* in our granule cell

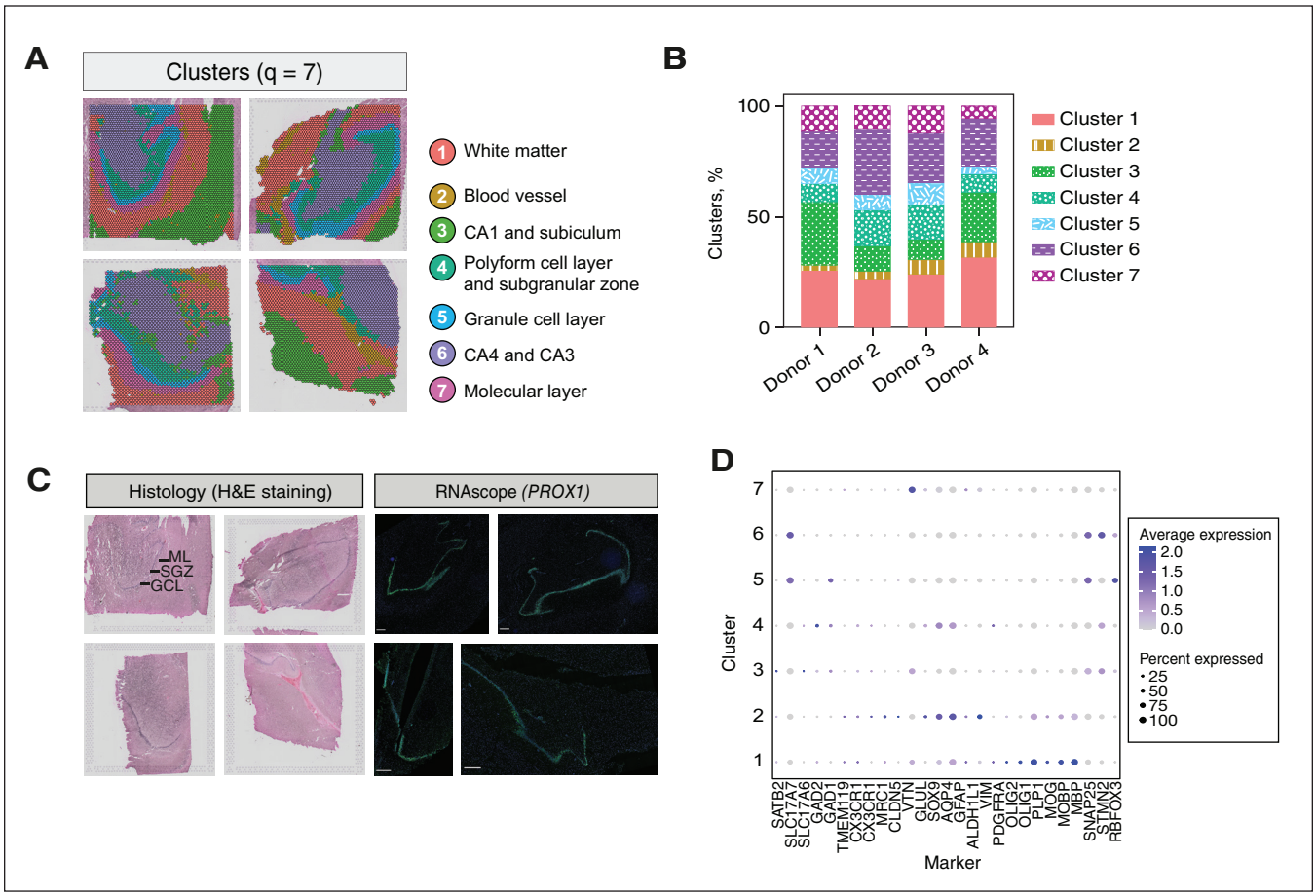

Figure 2: Detection of neurogenesis markers in Visium Spatial Gene Expression data of the adult human hippocampus. (A) Plots showing the 7 clusters (white matter, blood vessel, CA1 and subiculum, polyform cell layer and subgranular zone [SGZ], granule cell layer [GCL], CA3 and CA4, and molecular layer [ML]) generated with the BayesSpace *t*-distributed error model algorithm. Sections on the left are from middle-aged males (n = 2, mean age 42.5 yr), and sections on the right are from young adult males (n = 2, mean age 23.5 yr). (B) Percentage of spots in each of the 7 BayesSpace clusters in each section. Supporting data are presented in Appendix 1, Table 3. (C) Validation of dentate gyrus (DG) morphology with hematoxylin and eosin (H&E) staining and RNAscope using a probe directed against the *PROX1* (in green) dentate-lineage marker, with 4′,6-diamidino-2-phenylindole (DAPI) nuclear staining in blue (scale = 800 µm). The lines are labelling the SGZ, GCL, and ML of the DG. (D) Dotplot visualization of the scaled average expression of canonical cell-type marker genes in each BayesSpace cluster in all sections, including *SATB2*, *SLC17A7*, and *SLC17A6* (excitatory neurons); *GAD1* and *GAD2* (inhibitory neurons); *TMEM119*, *CX3CR1*, and *MRC1* (microglia); *CLDN5* and *VTN* (endothelial cells); *GLUL*, *SOX9*, *AQP4*, *GFAP*, *ALDH1L1*, and *VIM* (astrocytes); *PDGFRA*, *OLIG1*, and *OLIG2* (oligodendrocyte precursor cells); *PLP1*, *MOG*, *MOBP*, and *MBP* (oligodendrocytes); and *SNAP25*, *STMN2*, and *RBFOX3* (neurons). The size of the dot corresponds to the percentage of spots within a cluster enriched for the marker. The colour of the dot represents the scaled average expression levels of the marker across spots within a cluster. Supporting data are presented in Appendix 1, Table 4.

layer cluster (cluster 5), we assessed *GAD1*'s spatially resolved expression within each section and observed that the expression of the marker strongly mapped to the DG (Figure 3).

With multiplexed FISH (RNAscope), we validated the spatial distribution of markers that had low expression in the DG when assessed computationally with Visium (Figure 4). Similar to the spatial feature mappings, we found *DCX*-expressing and *NES*-expressing cells dispersed within the DG and outside the DG, and cells expressing *PCNA* outside the DG. Inversely, *MCM2* expression was virtually absent in both regions of interest (Figure 4).

In our differential gene expression analysis (Appendix 1, Supplementary Figure 3A), we identified 24 common genes (1.5% overlap) between DEGs in cluster 5 and DEGs identified by Wang and colleagues[19] and Zhou and colleagues[20] from immature neuronal clusters (Appendix 1, Supplementary Figure 3C, and Appendix 2, Table 4). Overlapping genes included *CD24*, previously found to be enriched in rodent immature granule neurons;[37,38] *NRGN*, involved in synaptic plasticity in the rodent hippocampus;[39] and *NCDN*, a regulator of adult hippocampal neurogenesis, identified in an earlier study in the rodent brain.[40] We also found overlap between

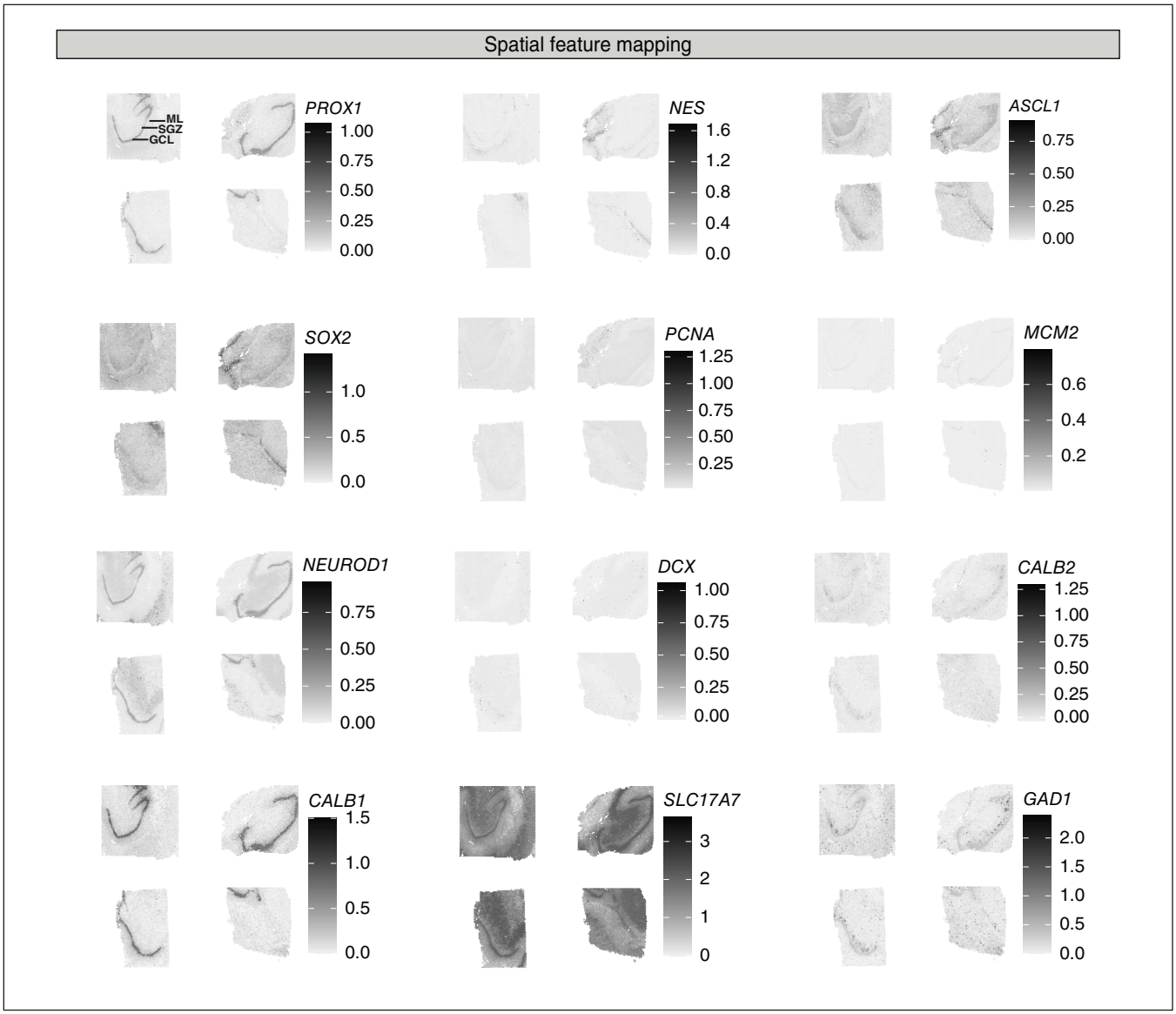

Figure 3: Detection of neurogenesis markers in Visium Spatial Gene Expression data of the adult human hippocampus, showing log-normalized expression of neurogenesis markers spatially plotted onto each section at the subspot level using BayesSpace, including *NES*, *SOX2*, and *ASCL1* (neural stem cells); *PCNA* and *MCM2* (proliferative cells); *NEUROD1* (neuroblasts); *DCX* and *CALB2* (immature granule neurons); *CALB1* (mature granule neurons); *PROX1* (dentate lineage cells); *SLC17A7* (excitatory neurons); and *GAD1* (inhibitory neurons). Higher values in the scale correspond to higher expression levels, whereas lower values reflect lower expression levels. Supporting data can be accessed using our data set, deposited in Gene Expression Omnibus and following our analysis steps.

the DEGs from cluster 4 and those from Wang and colleagues'[19] neural stem cell and astrocyte cluster (Appendix 1, Supplementary Figure 3D, and Appendix 2, Table 5). Among the 12 common genes were glial markers, such as *GFAP*, *ALDH1A1*, *AQP4*, and *GJA1* (Appendix 2, Table 5). Interestingly, 4 of the common genes — *PITPNC1*, *DTNA*, *NTRK2*, and *TNC* — were also found to be enriched in both astrocytes and neural stem cells in the adult rodent subgranular zone,[41] further revealing important transcriptomic similarities between astrocytic and neural stem cell populations within the hippocampal neurogenic niche.

A hippocampal cluster of 201 nuclei with a transcriptomic profile suggestive of neural stem cells was previously identified;[18] to better identify this cluster, we spatially reconstructed it, as well as other previously identified clusters with spot deconvolution (Figure 5 and Appendix 1, Supplementary Figures 4 and 5).[30] We observed that spots located in the granule cell layer had higher proportions (10%–20%) of the transcriptomic profile for the DG granule neuron cluster, whereas the predicted spatial location of the neural stem cell cluster did not correspond to the subgranular zone, but rather to regions outside of the DG. These results further support the recent re-analysis of the data set in which the authors re-examined the transcriptomic identity of the neural stem cell cluster by performing gene set enrichment using a set of previously identified human ependymal cell markers.[13,42]

We looked at the enrichment of different sets of genes identified in 3 other recent single-cell and single-nucleus RNA sequencing data sets of the developing[31] and adult human hippocampus[19,20] using gene signature scoring (Appendix 1, Supplementary Figure 6 and Appendix 2, Tables 2 and 3). Interestingly, we found that the DEGs of immature granule neurons identified by Zhou and colleagues[20] and Wang and colleagues[19] were enriched in excitatory neuronal clusters, whereas DEGs of the developing hippocampus identified by Zhong and colleagues[31] were enriched both within and outside the DG, with no clear enrichment in spots located in the neurogenic niche. Zhou and colleagues'[20] set of positive gene weights, used to identify immature granule neurons, was mostly enriched in cluster 5, located along the granule cell layer. Our integration of external genomic data sets with the Visium data demonstrates how differences in the processing and clustering of single-cell and single-nucleus RNA sequencing data sets can strongly influence the identification of neurogenic cell types.

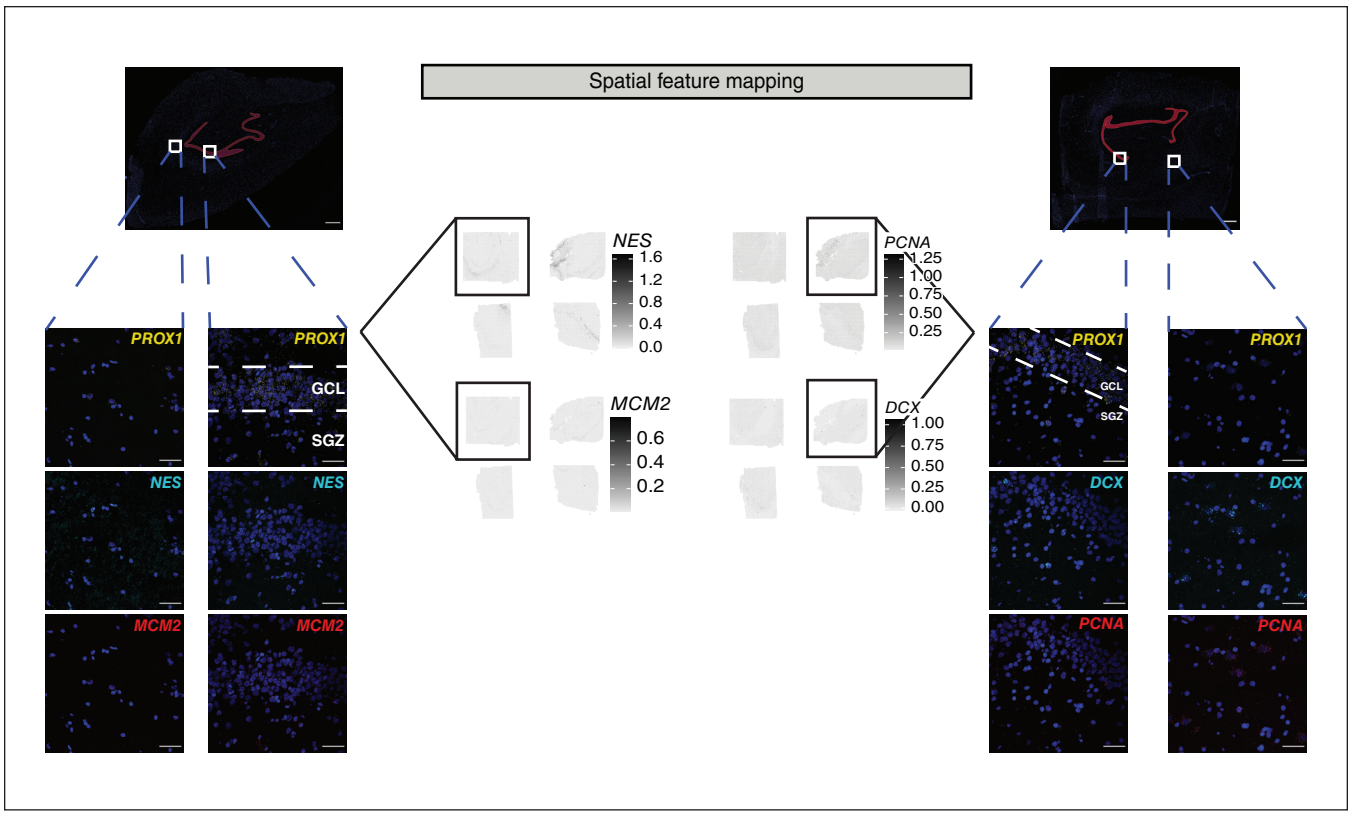

Figure 4: Qualitative comparison of gene expression between Visium and multiplexed fluorescent in situ hybridization (RNAscope) within and outside the dentate gyrus (DG). Enlarged sub-spot level plots showing *NES*, *PCNA*, *MCM2*, and *DCX* log-normalized expression on each section, with representative RNAscope images of *NES*, *PCNA*, *MCM2*, and *DCX* expression within and outside the DG from 2 samples. The delineated area in red corresponds to the subgranular zone (SGZ) and granule cell layer (GCL) on both sections (scale bars of whole DG sections = 1 mm; scale bars of expanded insets = 50 μm). Supporting data can be accessed using our data set, deposited in Gene Expression Omnibus and following our analysis steps.

Altogether, these data showed that neurogenesis markers were spatially resolved to cells in the DG. However, they also mapped to regions outside of the typical hippocampal neurogenic niche, which raises questions as to the specificity of these markers, especially immature neuronal markers, to adult hippocampal neurogenesis. Our findings showed the different patterns of expression of these markers, which have been commonly used in the literature to identify neurogenic cell types in the adult human DG and have sparked controversy regarding their expression levels at the protein level in the DG, as well as outside the neurogenic niche. They further confirm the importance of using multiple markers to characterize different neurogenic cell types in the human DG.

Expression of neural stem cell and proliferation markers, and the number of DCX+ cells in the adult human dentate gyrus from childhood to middle age

To investigate neurogenic cells at the transcriptomic level, we used multiplexed FISH in the subgranular zone and granule cell layer of hippocampal samples from 1 infant, 1 adolescent, and 6 adults (Figure 1 and Appendix 1, Table 2). Using a combination of probes to identify neural stem cells, we found very few *NES*$^{+}$*SOX2*$^{+}$ cells with or without expression of *ALDH1L1* in the subgranular zone, and almost none in the granule cell layer, of the adolescent and adults (Figure 6A), which is congruent with the immunohistochemistry-related findings of Boldrini and colleagues.[2] These presumed neural stem cells represented less than 1% of all subgranular zone cells in the adolescent and adult samples, although no statistically significant correlation was found between the percentage of these cells and age in each DG layer (Appendix 1, Supplementary Figure 7 and Appendix 3, Table 1, available at www.jpn.ca/lookup/doi/10.1503/jpn.240026/tab-related-content). We used *PCNA* and *MCM2* probes to estimate cell proliferation in the adult DG but were unable to quantify their expression levels since no more than 1 cell per DG section displayed a signal above threshold for either of these markers (Figure 6B). The low detection levels of these markers were consistent with their predicted spatial feature mapping (Figure 3).

The low combined expression of *NES*, *SOX2*, and *ALDH1L1*, as well as the low expression of *PCNA* and *MCM2* that we observed in all samples suggests that proliferation in the DG is either mostly or entirely completed prenatally. These findings are consistent with previous reports that suggested that proliferation in the human DG drops substantially during infancy[7] and that human DG development occurs prenatally.[43]

To address the debate of DCX-immunolabelled cells in the DG,[2,3,5–7,9,13] we labelled *DCX* transcripts in the subgranular zone and granule cell layer (Figure 6C). We found that *DCX*$^{+}$ cells in the granule cell layer decreased from an average of 44.1 (standard deviation [SD] 21.8) cells/mm^2 in the infant sample to an average of 8.9 (SD 4.1) cells/mm^2 in the adolescent sample, while *DCX*$^{+}$ cells in the subgranular zone remained similar across all age groups (Figure 6D; Appendix 1, Supplementary Figure 8A, 8B, and 8C; and Appendix 3, Table 2).

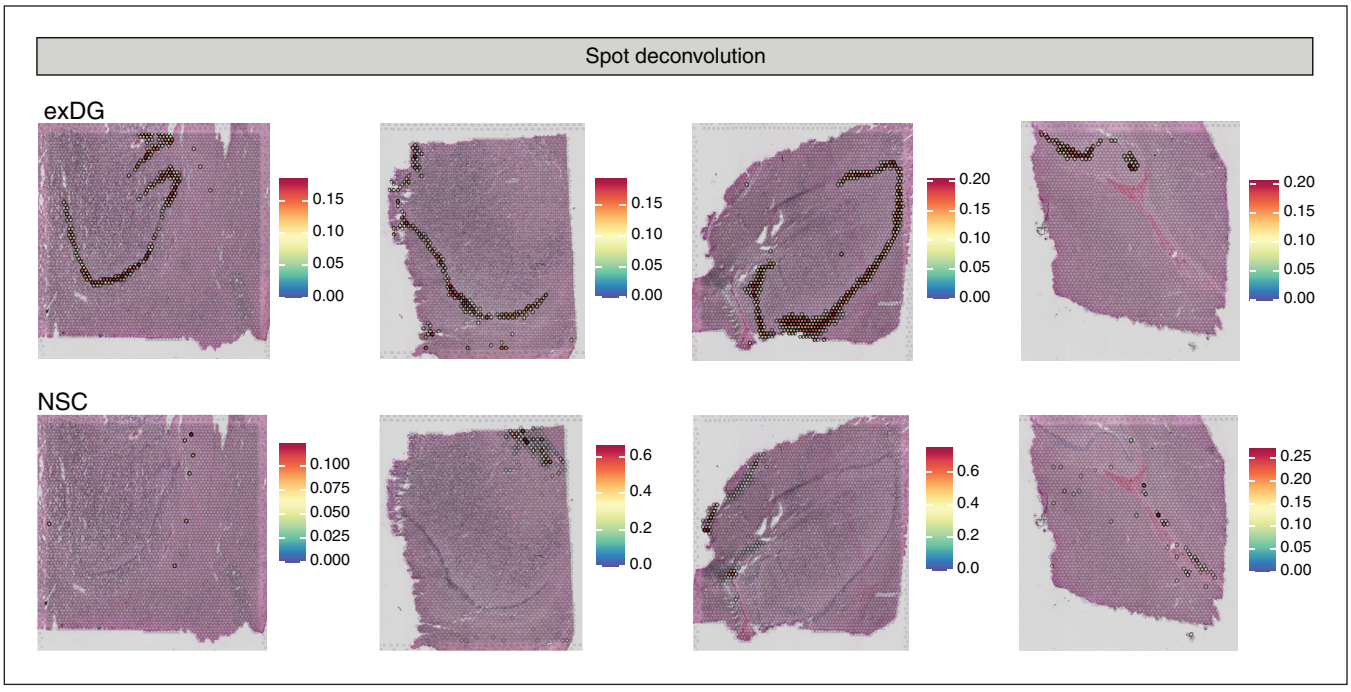

Figure 5: Spatial reconstruction of a human hippocampal single-nucleus RNA sequencing data set with spot deconvolution, including the dentate gyrus (DG) granule neuron (exDG)[18] and the neural stem cell (NSC) clusters from Habib and colleagues.[18] The coloured scale corresponds to the proportions of cell type markers from the single-nucleus clusters represented in each spot. DAPI = 4′,6-diamidino-2-phenylindole. Supporting data presented in Appendix 4, Tables 1 and 2, available at https://www.jpn.ca/lookup/doi/10.1503/jpn.240026/tab-related-content.

Phenotypes of DCX⁺ cells in the adult human dentate gyrus

We next investigated the possible phenotypes of *DCX*⁺ cells detected in hippocampal neurogenesis–associated layers of the adult DG by quantifying *DCX* expression with different cell type markers, namely *SLC17A7* (excitatory neurons), *GAD1* (inhibitory neurons), *NEUROD1* (neuroblasts), and *PROX1* (dentate lineage) (Figure 7A, 7B, and 7C). [34,35,44] Quantification of *SLC17A7* and *DCX* co-expression revealed a decrease in the percentage of *DCX*⁺ cells expressing

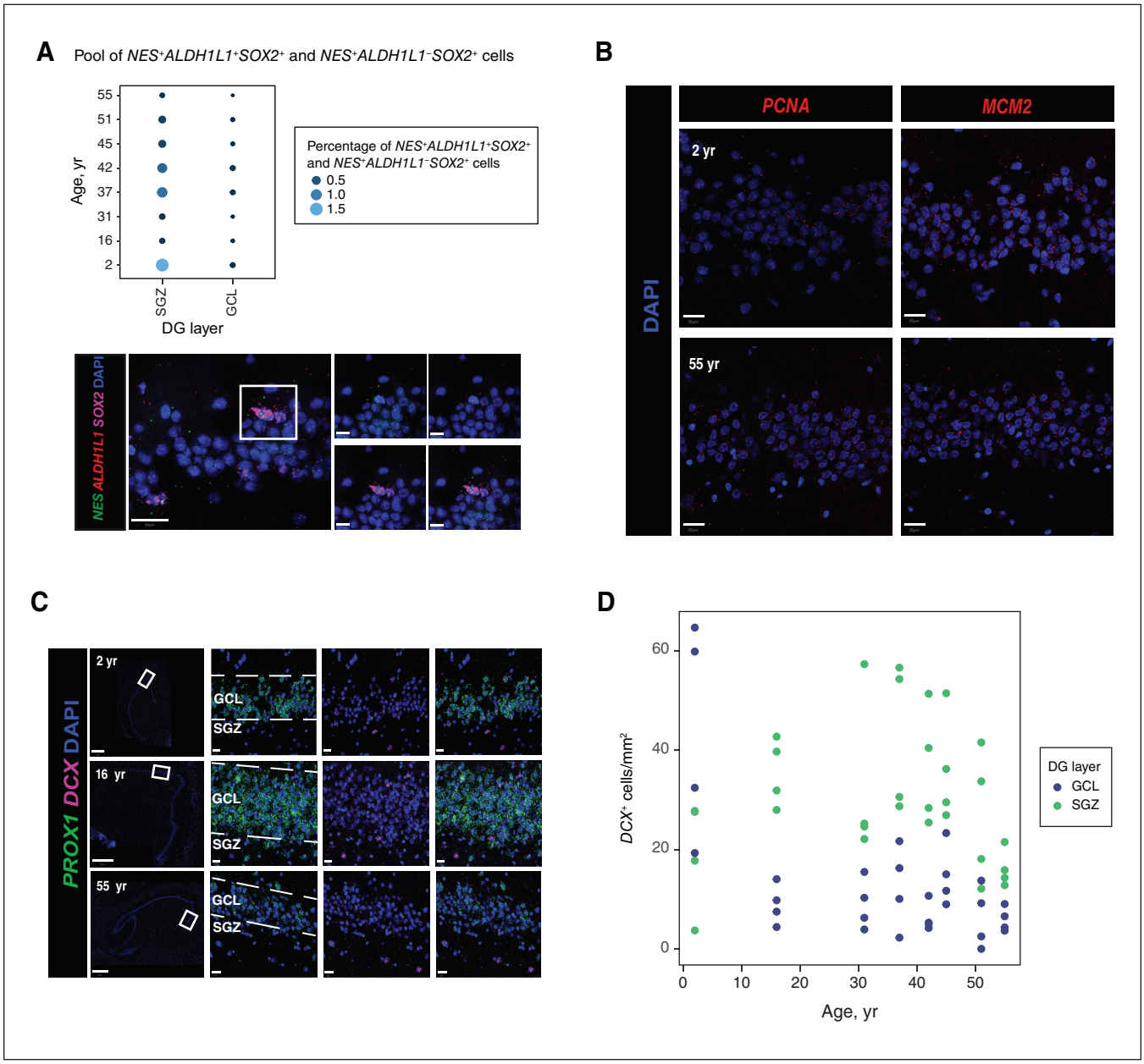

Figure 6: Distribution of neural stem cell and proliferation marker genes, and density of *DCX*⁺ cells in the subgranular zone (SGZ) and granule cell layer (GCL) of the human dentate gyrus (DG). (A) Percentage of *NES*⁺*SOX2*⁺ cells with or without *ALDH1L1* expression in the SGZ and GCL of the whole DG in samples from an infant, an adolescent, and 6 adults. The lower panel shows a *NES*⁺, *SOX2*⁺, and *ALDH1L1*⁺ cell in the GCL of the infant DG (age 2 yr). Scale bars indicate 20 μm (scale bars for expanded insets = 10 μm). Supporting data presented in Appendix 3, Table 1. (B) Expression of *PCNA* and *MCM2* in the infant (age 2 yr) and adult DG (age 55 yr). Scale bars indicate 20 μm. (C) *DCX* expression detected in *PROX1*⁺ and *PROX1*⁻ cells in the DG of different age groups. Scale bars indicate 1 mm (scale bars for expanded insets = 20 μm). Dotted lines delineate the SGZ and GCL of the DG. (D) Number of *DCX*⁺ cells/mm² in the SGZ and GCL of the whole DG in infant (*n* = 1, age 2 yr), adolescent (*n* = 1, age 16 yr), and adult (*n* = 6, mean age 43.5 yr) samples. The graph shows values of 4 staining replicates per participant. Supporting data presented in Appendix 3, Table 2. DAPI = 4′,6-diamidino-2-phenylindole.

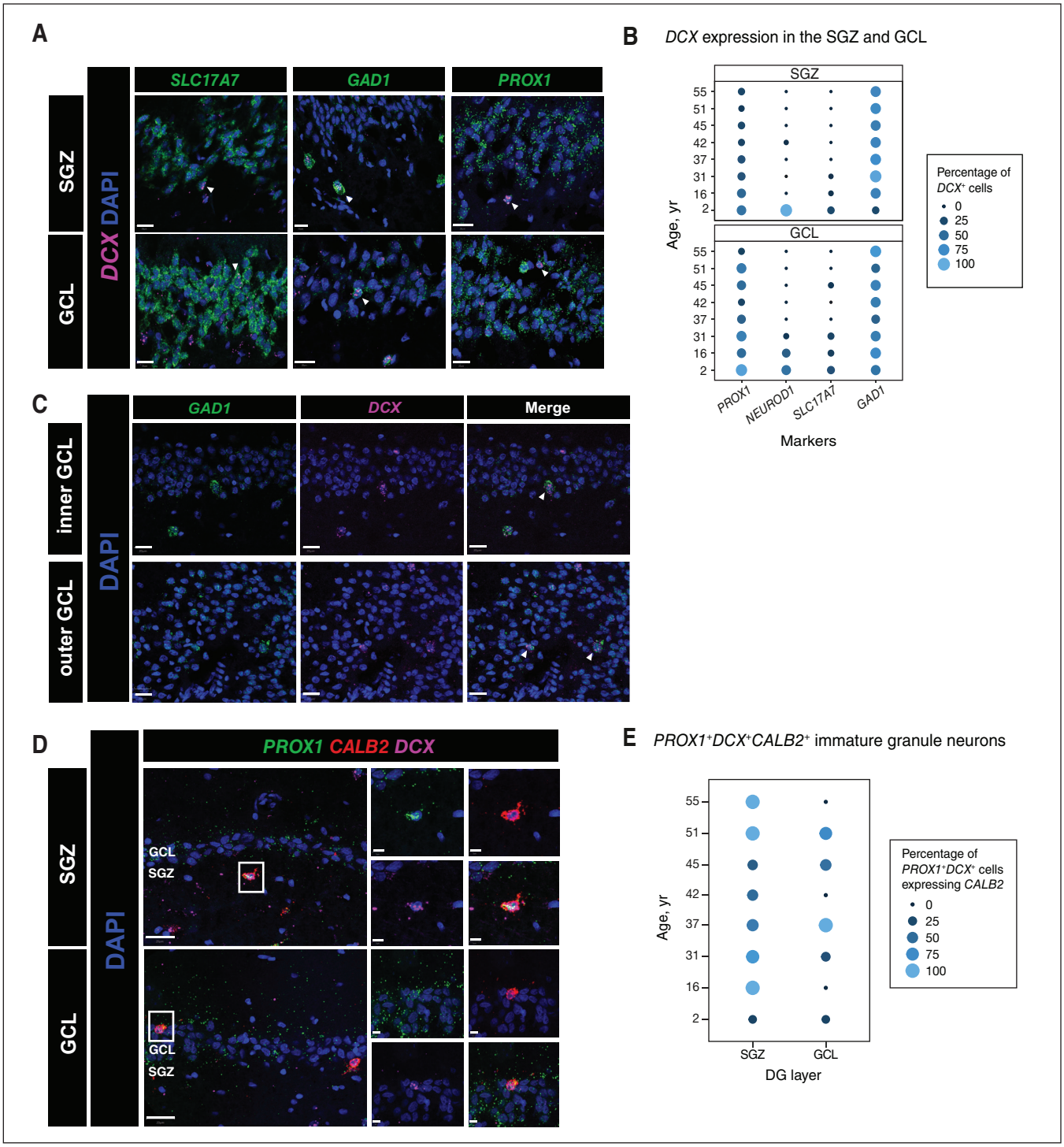

Figure 7: Distribution of *DCX* expression and different cell-type marker and immature neuronal genes in the subgranular zone (SGZ) and granule cell layer (GCL) of the human dentate gyrus (DG). (A) *DCX* expression detected in cells expressing *PROX1* (dentate lineage), *SLC17A7* (excitatory neurons), and *GAD1* (inhibitory neurons) in the SGZ and GCL of the DG from a 31-year-old adult (scale bars = 20 μm). (B) Percentage of *DCX*$^+$ cells expressing *PROX1*, *NEUROD1*, *SLC17A7*, and *GAD1* in the SGZ and GCL of the whole DG by participant age. Supporting data are presented in Appendix 3, Table 3. (C) *DCX*$^+$ and *GAD1*$^+$ cells located in the inner GCL (closer to the SGZ) and outer GCL (closer to the molecular layer) of a 55-year-old adult (scale bars = 20 μm). White arrows point to double-positive cells. (D) *DCX*$^+$ cells expressing *PROX1* and *CALB2* in the SGZ and GCL of the DG from a 37-year-old adult (scale bars = 20 μm; scale bars for expanded insets = 5 μm). (E) Percentage of *PROX1*$^+$ and *DCX*$^+$ cells expressing *CALB2* in the SGZ and GCL of the whole DG by participant age. Supporting data are presented in Appendix 3, Table 4. DAPI = 4′,6-diamidino-2-phenylindole.

SLC17A7 in both DG layers among adults (Figure 7B and Appendix 1, Supplementary Figure 8D and 8E). Strikingly, about half of *DCX*$^+$ cells were found to express *GAD1* in the subgranular zone and the granule cell layer among participants of all ages, with cells located either in the inner or outer granule cell layer, in the vicinity of the molecular layer (Figure 7B and 7C and Appendix 1, Supplementary Figure 8D and 8E). Conversely, the decline in the percentage of *DCX*$^+$ and *NEUROD1*$^+$ cells correlated with aging in both layers, becoming barely detectable in adults (Figure 7B and Appendix 1, Supplementary Figure 8D and 8E). Among adults, we found a decrease in the percentage of *DCX*$^+$ cells expressing the dentate lineage marker in both DG layers, although this correlation reached significance only in the subgranular zone (Figure 7B and Appendix 1, Supplementary Figure 8D and 8E). Our findings suggest that most *DCX*$^+$ cells in the adult human DG may display a GABAergic phenotype (average of 61% in the granule cell layer and 75% in the subgranular zone), whereas only a minority of *DCX*$^+$ cells were committed to a glutamatergic fate (average of 5% in the granule cell layer and 1% in the subgranular zone) (Appendix 3, Table 3). We also noted that a substantial subset of *DCX*$^+$ cells did not express *SLC17A7* or *GAD1*; these may represent immature neurons not yet committed to a particular phenotype. It is also possible that at least some of these *DCX*-expressing cells correspond to glial cells or to cells with multipotentiality, such as oligodendrocyte precursor cells.[7,13,45,46] Indeed, previous studies have reported DCX expression in cell types that are not part of the dentate lineage — including microglia and astrocytes — in the human brain.[7,47] Consistent with these findings, our results showed that *DCX* transcripts were detected in *TMEM119*$^+$ microglia and *ALDH1L1*$^+$ astrocytes in the adult human DG (Appendix 1, Supplementary Figure 9A and 9B).

To investigate the presence of a pool of immature granule neurons in the DG throughout normal aging, we used a combination of *PROX1*, *DCX*, and *CALB2* probes, based on previous studies (Figure 7D).[2,5,48,49] Quantification of these probes in the subgranular zone and granule cell layer revealed that most *PROX1*$^+$ and *DCX*$^+$ cells expressed *CALB2* in the subgranular zone among adults (average of 73%) (Figure 7E and Appendix 3, Table 4). In *PROX1*$^+$ and *DCX*$^+$ cells located in both layers of the DG in infant and adult hippocampi, we detected transcripts of *STMN1*, which encodes a tubulin-depolymerizing protein that is enriched in human immature granule neurons (Appendix 1, Supplementary Figure 10A and 10B, and Appendix 3, Table 5).[20] We also validated *STMN1* expression in the DG with our spatial transcriptomic data (Appendix 1, Supplementary Figure 10C).

DCX expression in non-neurogenic brain regions

Previous reports have shown expression of DCX in non-neurogenic regions, such as the human amygdala and cerebral cortex.[13,50–52] These findings raise concerns regarding the validity of *DCX* as an appropriate proxy for adult brain neurogenesis. To further confirm *DCX* expression in non-neurogenic regions, we first spatially mapped the expression of *DCX* and *PROX1* onto publicly available spatial genomic data of DLPFC sections.[27] We observed *DCX* expression in a few sub-spots in all 4 DLPFC sections, whereas *PROX1* was mainly expressed in sub-spots located in the cluster annotated as white matter (Figure 8A). These results confirmed that expression of these markers may be found outside of the neurogenic niche of the human DG, which is in agreement with our spatial transcriptomic findings (Figure 3). We also confirmed the presence of *DCX* expression in the *DLPFC* using FISH on frozen unfixed sections (Figure 8B).

In addition, we found *DCX*$^+$ cells in the molecular layer of the DG, a region where DCX-immunolabelled cells have been previously observed (Figure 8C).[17] Finally, we also detected *DCX* expression in other hippocampal areas, such as the CA3 (Figure 8D), as well as in *PROX1*$^+$ cells from regions highly expressing the oligodendrocyte-specific marker *MBP* (Figure 8E). These observations suggest that multipotential cells (e.g., oligodendrocyte precursor cells) expressing *DCX* could migrate out of the DG circuitry to reach their final destination and mature into the required cell type,[46] but this hypothesis requires further examination. Altogether, our data suggest that markers that are commonly used to examine adult hippocampal neurogenesis may be insufficient to specifically define neurogenic cell types as they are expressed in brain regions not known to be neurogenic.

Discussion

We examined adult hippocampal neurogenesis in samples of a wide age range; our findings provide important insights into the spatial expression of several neurogenesis markers, as well as the possible phenotypes of *DCX*$^+$ cells in the DG of the healthy human brain. Our findings indicated that the adult human DG exhibits, at most, very low levels of neurogenesis, given the scarcity of neural stem cells and lack of expression of proliferative markers. A summary of our main findings is presented in Figure 9. The association between high brain complexity and low hippocampal neurogenesis in humans is a paradoxical observation that has been highlighted in previous studies.[53,54]

Although our data suggest that DG neurogenesis is not a substantial phenomenon in humans postnatally, the small population of immature granule neurons in this region may play a more important role in driving hippocampal plasticity. Such cells have previously been suggested to contribute to the maintenance of a neurogenic reserve,[55] provide lifelong flexibility to the brain region, and act as a buffer against age-related hippocampal functional deficits.[55,56] It is therefore possible that, in the human DG, these immature granule neurons contribute substantially to preventing age-related brain damage.[57] Some experimental evidence supports this hypothesis in the adult rodent hippocampus;[58,59] however, future work should investigate the relevance of this hypothesis in the adult human DG.

Whether these immature granule neurons are newly generated or not remains unknown. However, we speculate that these immature neurons may have different origins, as previously stated in Seki.[11] Cells expressing immature neuronal markers may reflect neurons generated prenatally that persist during adulthood by remaining in a dormant-like state; neurons

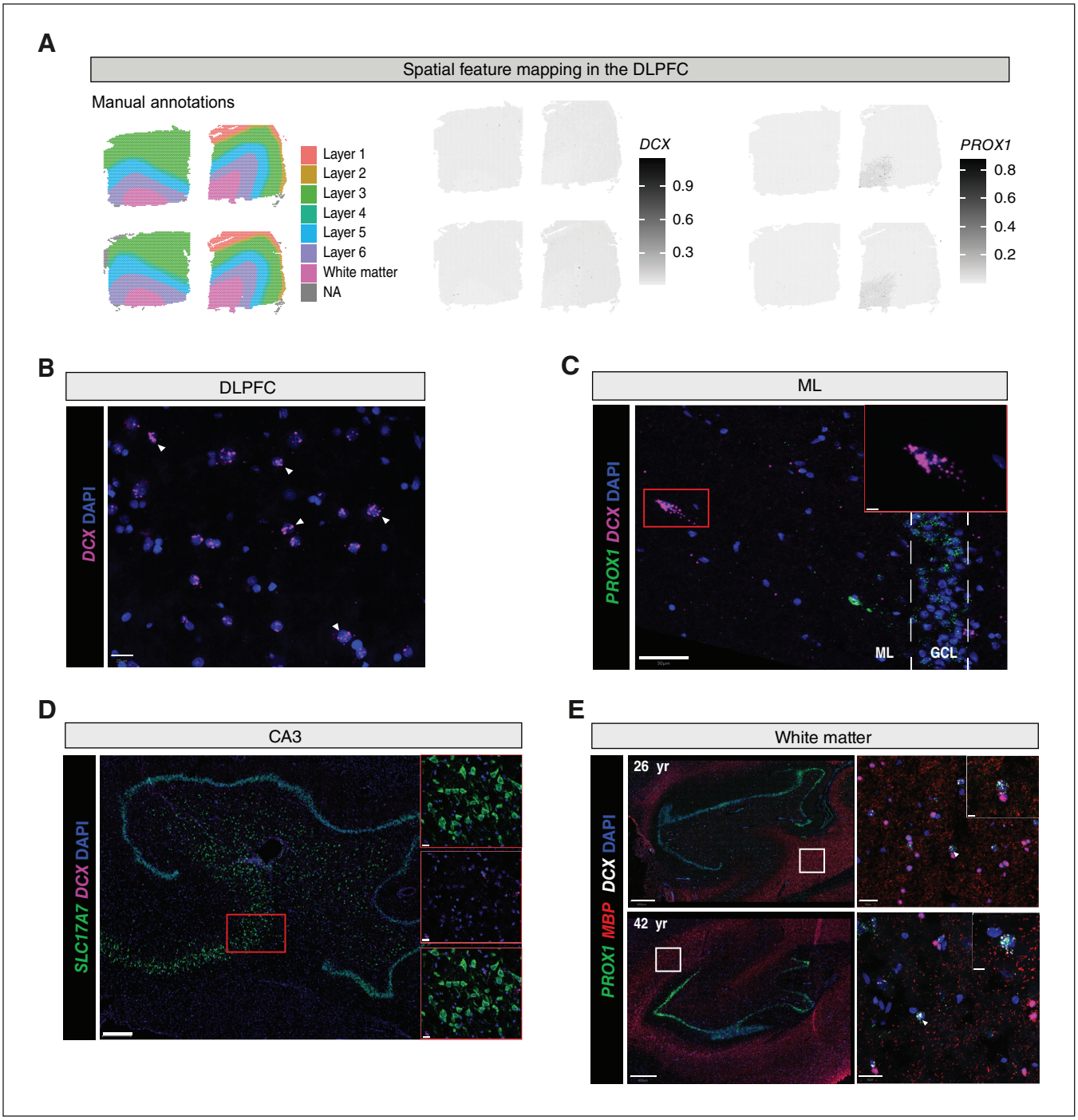

Figure 8: Specificity and distribution of *DCX* in the human brain. (A) Left panel shows manual annotations of samples 151671, 151672, 151673 and 151674 from Maynard and colleagues[27] (*n* = 4, 2 males and 2 females, mean age 38.41 yr), including the 6 cortical layers (layers 1–6) and a white-matter region. Middle and right panels show the log-normalized expression of *DCX* and *PROX1*, spatially plotted onto each section at the sub-spot level. Higher values in the scale correspond to higher expression levels, whereas lower values reflect lower expression levels. (B) *DCX* expression with 4′,6-diamidino-2-phenylindole (DAPI) staining in a dorsolateral prefrontal cortex (DLPFC) section of a 26-year-old adult (scale bars = 50 μm). White arrows point to *DCX*$^+$ cells. (C) *DCX* expression detected in the molecular layer (ML) of the dentate gyrus (DG) of a 37-year-old adult (scale bars = 50 μm; scale bars of expanded inset = 10 μm). (D) *DCX* expression in cells located in the CA3 region of the hippocampus in a 51-year-old adult (whole DG slide scanner images with scale bar = 500 μm; scale bars; higher magnification confocal images scale bars = 20 μm). (E) *DCX* expression in *PROX1*$^+$ cells located in highly *MBP*-expressing regions in the adult human hippocampus (whole DG slide scanner images with scale bars = 800 μm; higher magnification confocal images with scale bars = 20 μm [5 μm for expanded insets]). GCL = granule cell layer; NA = not available.

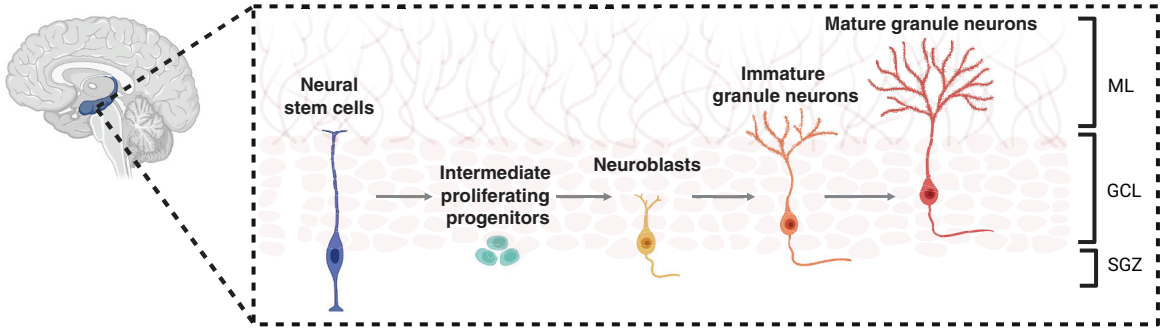

Cell type	10x Genomics Visium Spatial Gene Expression	Multiplexed fluorescent in situ hybridization (RNAscope)
Neural stem cells	• *NES* and *SOX2* are expressed in regions enriched for astrocytic and OPC markers.	• There are very few *NES*$^+$*SOX2*$^+$ cells (expressing *ALDH1L1* or not) in the adult DG.
Intermediate proliferating progenitors	• *PCNA* and *MCM2* are lowly expressed in the adult DG.	• There is an absence of *PCNA*- and *MCM2*-expressing cells in the DG.
Neuroblasts	• *NEUROD1* expression is clustered along the GCL of the adult DG.	• Very few *NEUROD1*$^+$*DCX*$^+$ cells are present in the adult DG.
Immature granule neurons	• *PROX1*, *CALB2*, and *DCX* are expressed within and outside the DG. • *DCX* is widely distributed within the DG. • *STMN1* expression is not specific to the DG. • The top DEGs of cluster 5 include *NCDN, CD24, GABRQ, PHYHIP*, and *PPP1R1A*.	• Most *DCX*-expressing cells are GABAergic (*GAD1*$^+$). • Cells expressing *PROX1*, *CALB2*, and *DCX* are present in the adult DG. • Cells expressing *PROX1*, *STMN1*, and *DCX* are present in the adult DG.

Figure 9: Graphical representation of the the main findings from Visium and RNAscope. See Related Content tab for accessible version. DEG = differentially expressed gene; DG = dentate gyrus; GCL = granule cell layer; ML = molecular layer; OPC = oligodendrocyte precursor cell; SGZ = subgranular zone. Figure created with BioRender (www.biorender.com).

generated postnatally that are a result of minimal proliferation in the DG and remain in a prolonged state of immaturity, which corroborates the idea of a delayed maturation of immature dentate granule neurons, thought to occur in long-living and large-brained species;[57,60,61] and neurons that are re-expressing immature neuronal markers, according to the recent hypothesis of neuronal dematuration in the DG.[11,62]

The expression of *GAD1* in *DCX*$^+$ cells in the granule cell layer was an unexpected finding. Although an earlier study reported weak immunoreactivity for GAD1 in granule cell layer neurons in the healthy human DG,[63] rodent studies have identified and characterized Gad1 expression in the granule cell layer and, more precisely, in the inner part of the layer adjacent to the subgranular zone,[64,65] suggesting that Gad1$^+$ cells displaying an immature phenotype in this layer are undergoing late neuronal differentiation.[64] Similarly, another study detected colocalization of DCX and GAD1 in DG granule cells from younger and older human participants.[66] Thus, it is plausible that most of the *DCX*-expressing cells of the granule cell layer that we identified are in a late granule cell differentiation stage since the number of *DCX*$^+$ cells expressing *NEUROD1*, an early neuronal differentiation marker,[44] decreases in the DG of older adults, while the number of *DCX*$^+$ cells expressing *GAD1* remains high. The present identification of *GAD1*$^+$*DCX*$^+$ cells in the granule cell layer across all samples confirms the presence of this subpopulation and warrants further investigation of their functional properties.

Limitations

The scope of this study was limited to mRNA detection of various neurogenesis markers in the DG. Our spatial transcriptomic experiments, as well as our in situ hybridization studies involved small sample sizes and included only males. Future research should focus on sex-specific differences in the number of cells expressing markers of stemness, proliferation, and neuronal immaturity in the adult DG, and their levels of expression (both computationally and in situ). Despite these limitations, our results provide support for the hypothesis that the neurogenic capacity of the adult human DG may rely primarily on a reserve of immature granule neurons.

Conclusion

Understanding the functional importance of the presence of a population of immature granule neurons during physiologic aging can propel future research on how DG

neuroplasticity is altered in brain disorders and in response to stress, more particularly in the context of mental illness.

Acknowledgements: The authors thank Dominique Mirault and Zhipeng Niu for technical assistance, and Dr. Nada Jabado for providing one of the brain samples used in this study.

Affiliations: From the McGill Group for Suicide Studies, Douglas Mental Health University Institute, McGill University, Montréal, Que. (Simard, Rahimian, Antonietta, Théberge, Turecki, Nagy, Mechawar); the School of Medical Sciences, Faculty of Medicine and Health, Charles Perkins Centre, The University of Sydney, Camperdown, Australia (Matosin); the Department of Psychiatry, McGill University, Montréal, Que. (Turecki, Nagy, Mechawar).

Competing interests: None declared.

Contributors: Natalie Matosin, Gustavo Turecki, Corina Nagy, and Naguib Mechawar contributed to study conception. Sophie Simard, Reza Rahimian, Maria Antonietta Davoli, and Corina Nagy contributed to study design. Sophie Simard and Stéphanie Théberge contributed to data analysis. All of the authors contributed to data interpretation. Sophie Simard and Naguib Mechawar drafted the manuscript. All of the authors revised it critically for important intellectual content, gave final approval of the version to be published, and agreed to be accountable for all aspects of the work.

Data sharing: The raw and processed Visium Spatial Gene Expression data and combined Seurat objects are deposited at National Center for Biotechnology Information's Gene Expression Omnibus (GSE248545) and are publicly available. Any additional information required to reanalyze the data reported in this work paper is available from the corresponding author upon request.

Funding: This work was funded by a Healthy Brains, Healthy Lives (HBHL) Innovative Ideas grant to Naguib Mechawar. Reza Rahimian received postdoctoral fellowships from Fonds de Recherche du Québec – Santé (FRQ-S) and the Adversity & Mental Health Initiative. The Douglas-Bell Canada Brain Bank is funded by platform support grants to Gustavo Turecki and Naguib Mechawar from the Réseau québécois sur le suicide, les troubles de l'humeur et les troubles associés (FRQ-S), HBHL, and Brain Canada.

References

1. Eriksson PS, Perfilieva E, Björk-Eriksson T, et al. Neurogenesis in the adult human hippocampus. *Nat Med* 1998;4:1313-7.
2. Boldrini M, Fulmore CA, Tartt AN, et al. Human hippocampal neurogenesis persists throughout aging. *Cell Stem Cell* 2018;22:589-99.e5.
3. Dennis CV, Suh LS, Rodriguez ML, et al. Human adult neurogenesis across the ages: an immunohistochemical study. *Neuropathol Appl Neurobiol* 2016;42:621-38.
4. Flor-Garcia M, Terreros-Roncal J, Moreno-Jimenez EP, et al. Unraveling human adult hippocampal neurogenesis. *Nat Protoc* 2020;15:668-93.
5. Moreno-Jimenez EP, Flor-Garcia M, Terreros-Roncal J, et al. Adult hippocampal neurogenesis is abundant in neurologically healthy subjects and drops sharply in patients with Alzheimer's disease. *Nat Med* 2019;25:554-60.
6. Seki T, Hori T, Miyata H, et al. Analysis of proliferating neuronal progenitors and immature neurons in the human hippocampus surgically removed from control and epileptic patients. *Sci Rep* 2019;9:18194.
7. Sorrells SF, Paredes MF, Cebrian-Silla A, et al. Human hippocampal neurogenesis drops sharply in children to undetectable levels in adults. *Nature* 2018;555:377-81.
8. Terreros-Roncal J, Moreno-Jiménez EP, Flor-García M, et al. Impact of neurodegenerative diseases on human adult hippocampal neurogenesis. *Science* 2021;374:1106-13.
9. Tobin MK, Musaraca K, Disouky A, et al. Human hippocampal neurogenesis persists in aged adults and alzheimer's disease patients. *Cell Stem Cell* 2019;24:974-82.e3.
10. Terstege DJ, Addo-Osafo K, Campbell Teskey G, et al. New neurons in old brains: implications of age in the analysis of neurogenesis in post-mortem tissue. *Mol Brain* 2022;15:38.
11. Seki T. Understanding the real state of human adult hippocampal neurogenesis from studies of rodents and non-human primates. *Front Neurosci* 2020;14:839.
12. Lucassen PJ, Toni N, Kempermann G, et al. Limits to human neurogenesis—really? *Mol Psychiatry* 2020;25:2207-9.
13. Sorrells SF, Paredes MF, Zhang Z, et al. Positive controls in adults and children support that very few, if any, new neurons are born in the adult human hippocampus. *J Neurosci* 2021;41:2554-65.
14. Moreno-Jimenez EP, Terreros-Roncal J, Flor-Garcia M, et al. Evidences for adult hippocampal neurogenesis in humans. *J Neurosci* 2021;41:2541-53.
15. Tartt AN, Fulmore CA, Liu Y, et al. Considerations for assessing the extent of hippocampal neurogenesis in the adult and aging human brain. *Cell Stem Cell* 2018;23:782-3.
16. Ayhan F, Kulkarni A, Berto S, et al. Resolving cellular and molecular diversity along the hippocampal anterior-to-posterior axis in humans. *Neuron* 2021;109:2091-105.e6.
17 Franjic D, Skarica M, Ma S, et al. Transcriptomic taxonomy and neurogenic trajectories of adult human, macaque, and pig hippocampal and entorhinal cells. *Neuron* 2022;110:452-69.e14.
18. Habib N, Avraham-Davidi I, Basu A, et al. Massively parallel single-nucleus RNA-seq with DroNc-seq. *Nat Methods* 2017;14:955-8.
19. Wang W, Wang M, Yang M, et al. Transcriptome dynamics of hippocampal neurogenesis in macaques across the lifespan and aged humans. *Cell Res* 2022;32:729-43.
20. Zhou Y, Su Y, Li S, et al. Molecular landscapes of human hippocampal immature neurons across lifespan. *Nature* 2022;607:527-33.
21. Simard S, Matosin N, Mechawar N. Adult hippocampal neurogenesis in the human brain: updates, challenges, and perspectives. *Neuroscientist* 2024 May 17 [Epub ahead of print]. doi: 10.1177/10738584241252581.
22. Ding SL, Royall JJ, Sunkin SM, et al. Comprehensive cellular-resolution atlas of the adult human brain. *J Comp Neurol* 2016;524:3127-481.
23. *Team RCR. A language and environment for statistical computing*. Vienna (Austria): R Foundation for Statistical Computing; 2021.
24. Hao Y, Hao S, Andersen-Nissen E, et al. Integrated analysis of multimodal single-cell data. *Cell* 2021;184:3573-87e29.
25. Scrucca L, Fop M, Murphy TB, et al. mclust 5: Clustering, classification and density estimation using gaussian finite mixture models. *R J* 2016;8:289-317.
26. Zhao E, Stone MR, Ren X, et al. Spatial transcriptomics at subspot resolution with BayesSpace. *Nat Biotechnol* 2021;39:1375-84.
27. Maynard KR, Collado-Torres L, Weber LM, et al. Transcriptome-scale spatial gene expression in the human dorsolateral prefrontal cortex. *Nat Neurosci* 2021;24:425-36.
28. Pardo B, Spangler A, Weber LM, et al. spatialLIBD: an R/Bioconductor package to visualize spatially-resolved transcriptomics data. *BMC Genomics* 2022;23:434.
29. Oliveros JC. Venny. *An interactive tool for comparing lists with Venn's diagrams*; 2007-2015. Available: https://bioinfogp.cnb.csic.es/tools/venny/index.html (accessed 2024 May 1).
30. Elosua-Bayes M, Nieto P, Mereu E, et al. SPOTlight: seeded NMF regression to deconvolute spatial transcriptomics spots with single-cell transcriptomes. *Nucleic Acids Res* 2021;49:e50.
31. Zhong S, Ding W, Sun L, et al. Decoding the development of the human hippocampus. *Nature* 2020;577:531-6.
32. Bankhead P, Loughrey MB, Fernández JA, et al. QuPath: Open source software for digital pathology image analysis. *Sci Rep* 2017;7:16878.
33. Wickham H. ggplot2: Elegant graphics for data analysis. Springer Cham; 2016:260.
34. Iwano T, Masuda A, Kiyonari H, et al. Prox1 postmitotically defines dentate gyrus cells by specifying granule cell identity over CA3 pyramidal cell fate in the hippocampus. *Development* 2012;139:3051-62.

35. Gao Z, Ure K, Ables JL, et al. Neurod1 is essential for the survival and maturation of adult-born neurons. *Nat Neurosci* 2009;12:1090-2.
36. von Bohlen und Halbach O. Immunohistological markers for proliferative events, gliogenesis, and neurogenesis within the adult hippocampus. *Cell Tissue Res* 2011;345:1-19.
37. Calaora V, Chazal G, Nielsen PJ, et al. mCD24 expression in the developing mouse brain and in zones of secondary neurogenesis in the adult. *Neuroscience* 1996;73:581-94.
38. Wang H, Zhou XM, Xu WD, et al. Inhibition of elevated hippocampal CD24 reduces neurogenesis in mice with traumatic brain injury. *J Surg Res* 2020;245:321-9.
39. Xiang Y, Xin J, Le W, et al. Neurogranin: a potential biomarker of neurological and mental diseases. *Front Aging Neurosci* 2020;12:584743.
40. Wang H, Warner-Schmidt J, Varela S, et al. Norbin ablation results in defective adult hippocampal neurogenesis and depressive-like behavior in mice. *Proc Natl Acad Sci U S A* 2015;112:9745-50.
41. Borrett MJ, Innes BT, Tahmasian N, et al. A shared transcriptional identity for forebrain and dentate gyrus neural stem cells from embryogenesis to adulthood. *eNeuro* 2022;9.
42. Kelley KW, Nakao-Inoue H, Molofsky AV, et al. Variation among intact tissue samples reveals the core transcriptional features of human CNS cell classes. *Nat Neurosci* 2018;21:1171-84.
43. Snyder JS. Recalibrating the relevance of adult neurogenesis. *Trends Neurosci* 2019;42:164-78.
44. Roybon L, Hjalt T, Stott S, et al. Neurogenin2 directs granule neuroblast production and amplification while NeuroD1 specifies neuronal fate during hippocampal neurogenesis. *PLoS One* 2009;4:e4779.
45. Walker TL, Yasuda T, Adams DJ, et al. The doublecortin-expressing population in the developing and adult brain contains multipotential precursors in addition to neuronal-lineage cells. *J Neurosci* 2007;27:3734-42.
46. Boulanger JJ, Messier C. Doublecortin in oligodendrocyte precursor cells in the adult mouse brain. *Front Neurosci* 2017;11:143.
47. Verwer RW, Sluiter AA, Balesar RA, et al. Mature astrocytes in the adult human neocortex express the early neuronal marker doublecortin. *Brain* 2007;130:3321-35.
48. Brandt MD, Jessberger S, Steiner B, et al. Transient calretinin expression defines early postmitotic step of neuronal differentiation in adult hippocampal neurogenesis of mice. *Mol Cell Neurosci* 2003;24:603-13.
49. Lavado A, Lagutin OV, Chow LM, et al. Prox1 is required for granule cell maturation and intermediate progenitor maintenance during brain neurogenesis. *PLoS Biol* 2010;8.
50. Li YN, Hu DD, Cai XL, et al. Doublecortin-expressing neurons in human cerebral cortex layer ii and amygdala from infancy to 100 years old. *Mol Neurobiol* 2023;60:3464-85.
51. Liu JYW, Matarin M, Reeves C, et al. Doublecortin-expressing cell types in temporal lobe epilepsy. *Acta Neuropathol Commun* 2018;6:60.
52. Sorrells SF, Paredes MF, Velmeshev D, et al. Immature excitatory neurons develop during adolescence in the human amygdala. *Nat Commun* 2019;10:2748.
53. Duque A, Arellano JI, Rakic P. An assessment of the existence of adult neurogenesis in humans and value of its rodent models for neuropsychiatric diseases. *Mol Psychiatry* 2022;27:377-82.
54. Augusto-Oliveira M, Arrifano GPF, Malva JO, et al. Adult hippocampal neurogenesis in different taxonomic groups: possible functional similarities and striking controversies. *Cells* 2019;8:125.
55. Kempermann G. The neurogenic reserve hypothesis: what is adult hippocampal neurogenesis good for? *Trends Neurosci* 2008;31:163-9.
56. Kempermann G, Gage FH, Aigner L, et al. Human adult neurogenesis: evidence and remaining questions. *Cell Stem Cell* 2018;23:25-30.
57. La Rosa C, Ghibaudi M, Bonfanti L. Newly generated and non-newly generated "immature" neurons in the mammalian brain: a possible reservoir of young cells to prevent brain aging and disease? *J Clin Med* 2019;8:685.
58. Merkley CM, Jian C, Mosa A, et al. Homeostatic regulation of adult hippocampal neurogenesis in aging rats: long-term effects of early exercise. *Front Neurosci* 2014;8:174.
59. Shevtsova O, Tan YF, Merkley CM, et al. Early-age running enhances activity of adult-born dentate granule neurons following learning in rats. *eNeuro* 2017;4:ENEURO.0237-17.2017.
60. Kohler SJ, Williams NI, Stanton GB, et al. Maturation time of new granule cells in the dentate gyrus of adult macaque monkeys exceeds six months. *Proc Natl Acad Sci U S A* 2011;108:10326-31.
61. Ngwenya LB, Peters A, Rosene DL. Maturational sequence of newly generated neurons in the dentate gyrus of the young adult rhesus monkey. *J Comp Neurol* 2006;498:204-16.
62. Hagihara H, Murano T, Ohira K, et al. Expression of progenitor cell/immature neuron markers does not present definitive evidence for adult neurogenesis. *Mol Brain* 2019;12:108.
63. Schwab C, Yu S, Wong W, et al. GAD65, GAD67, and GABAT immunostaining in human brain and apparent GAD65 loss in Alzheimer's disease. *J Alzheimers Dis* 2013;33:1073-88.
64. Cabezas C, Irinopoulou T, Cauli B, et al. Molecular and functional characterization of GAD67-expressing, newborn granule cells in mouse dentate gyrus. *Front Neural Circuits* 2013;7:60.
65. Zhao S, Zhou Y, Gross J, et al. Fluorescent labeling of newborn dentate granule cells in GAD67-GFP transgenic mice: a genetic tool for the study of adult neurogenesis. *PLoS One* 2010;5:e12506.
66. Knoth R, Singec I, Ditter M, et al. Murine features of neurogenesis in the human hippocampus across the lifespan from 0 to 100 years. *PLoS One* 2010;5:e8809.